FLiNaK Compatibility Studies with Alloy 600 and Silicon Carbide

Graydon L. Yoder, Jr.
Dennis Heatherly
Dane Wilson
Oak Ridge National Laboratory
Bldg. 5700, MS 6167
Bethel Valley Rd.
Oak Ridge, TN 37831
United States

Mario Caja
Electrochemical Systems, Inc. (ESI)
9320 Collingwood Rd.
Knoxville, TN 37922
United States

Abstract

A small liquid fluoride salt test apparatus has been constructed and testing has been conducted to examine the compatibility of silicon carbide (SiC), Alloy 600 and a spiral wound gasket material in FLiNaK, the ternary eutectic alkali metal fluoride salt mixture. These tests were conducted to evaluate materials and sealing systems that could be used in fluoride salt systems. Three months of testing at 700°C was conducted to assure that these materials and seals would be acceptable when operating under prototypic operating conditions. The SiC specimens showed little or no change over the test period, while the spiral wound gasket material did not show any degradation except that salt might have been seeping into the outermost spirals of the gasket. The Alloy 600 specimens showed regions of voiding which penetrated the specimen surface to about 250 μm in depth. Analysis indicated that the salt had leached chrome from the metal surface, as was expected for this material.

Keywords: Molten salt, liquid salt, corrosion, advanced reactor, component testing, experiment

1.0 Introduction

The fluoride salt cooled high temperature reactor (FHR) is being designed to provide a high temperature energy source for commercial electrical power, industrial heat, or hydrogen production. Various versions of the FHR exist (Bardett et al., 2009, Greene et al. 2010, Varma et al., 2012), but all near-term designs operate at a temperature of about 700°C and use FLiBe salt coolant. FliBe is a molten salt made from a mixture of lithium fluoride (LiF) and beryllium fluoride (BeF_2). FHR designs also use a tristructural-isotropic (TRISO) fuel system, centrifugal pumps for normal operation and natural circulation for decay heat removal, core structural materials of graphite and silicon carbide and nickel-based alloys in contact with the salt. A significant amount of testing must be performed on these designs to prove they are operable, safe and economic.

Extensive materials research and development was undertaken during the 1960s and 1970s as part of the Molten Salt Reactor Program to develop a material compatible with fluoride salts. The material developed, INOR-8, served as the containment material for the Molten Salt Reactor Experiment (MSRE) because of its corrosion resistance to fluoride salt and its attractive neutronic properties. This material was later commercialized by what is now known as Haynes International and called Hastelloy®-N. Hastelloy®-N is a nickel-molybdenum alloy with low chromium content, ensuring its corrosion resistance to fluoride salts, which tend to deplete the chromium in the metal. This depletion significantly decreases material integrity. Hastelloy®-N remains a commercial product, but it is not readily available in the forms needed for experiment construction and it is not economically viable for use in small quantities. A material very similar to Hastelloy®-N—MONICR— has been experimentally produced by SKODA Nuclear Machinery Company. MONICR has been tested in a liquid fluoride salt environment (Uhlir et al., 2012) with results similar to that of Hastelloy®-N. However, because MONICR was produced only in experimental quantities, it is not readily

available. Another alloy with similar chemistry to Hastelloy®-N is also being developed in China to support their fluoride salt reactor projects. However, this alloy is also not readily available at this time.

The testing described herein was designed to support the construction of a liquid salt test loop (LSTL) at ORNL. Ultimately, because of the availability and cost issues associated with Hastelloy®-N, Alloy 600 was chosen as a relatively common high temperature nickel alloy with relatively low chromium content (~14–17%) that would provide a sufficient lifetime for the LSTL. Part of the LSTL salt boundary (test section flow channel) is made of SiC with two points in the loop requiring seals that act as a salt boundary. These seals use spiral wound gaskets (Flexitallic) made of alternating grafoil and nickel layers. Additionally, the initial LSTL test article simulates a pebble fuel design and it uses graphite spheres to simulate the pebble bed. Therefore, there are four materials in the LSTL that are in contact with the salt: Alloy 600, grafoil, SiC and graphite. Because of issues associated with handling and storing beryllium-containing materials, a surrogate salt was chosen for use in LSTL testing. FLiNaK, a eutectic salt consisting of 46.5% LiF, 11.5% NaF and 42% KF, has thermophysical properties very similar to those of FLiBe and it serves as a good surrogate for FLiBe for thermal/fluid experimentation. A complete description of the LSTL facility can be found in Yoder et al. (2010, 2011 and 2012).

Testing was undertaken in support of the LSTL to evaluate the four materials that would be in contact with FLiNaK. Testing included all of these materials exposed to FLiNaK salt at 700°C in a cell type test apparatus for three months. This paper discusses the test apparatus, the tests performed and the test results.

2.0 Cell Design

A 3-D schematic of the experimental cell is depicted in Figure 1, which shows the cell inserted into an electrically heated furnace used to maintain cell temperatures. A nickel crucible holds the liquid salt and is located inside an outer stainless steel vessel that is used to maintain the correct inert atmosphere. The nickel crucible is 30.5 cm long and 12.7 cm in diameter and held approximately 3.5 l of salt during testing. An argon cover gas is used over the salt and a small argon flow rate is maintained to continuously sweep that area. A three-junction thermocouple probe allows salt temperature measurement at three axial locations. Four thermocouples located inside the

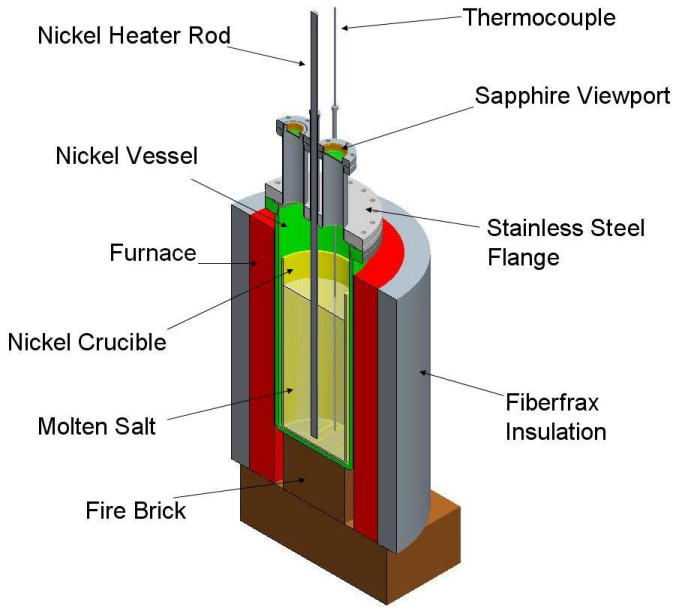

Figure 1 Schematic of molten salt cell.

heater system are used to measure heater surface temperature during operation. The thermocouple probe was fabricated by Delta-M Corporation and has nickel as the outer sheath material. Temperature measurement errors were estimated from the thermocouple calibration curves to be 0.55°C (a 1σ value). Two flange designs were used at the top of the cell. Both included two Sapphire viewports to allow visualization of the salt during testing

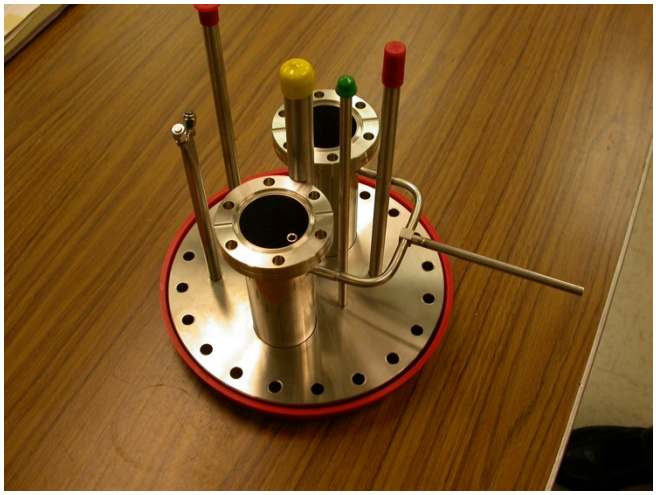

Figure 3 Upper flange of cell.

Some of the cell components are shown in the figures below. The two upper flange assemblies are made of stainless steel. Figure 2 shows the first top flange. The two large ports shown in the picture allow viewing of the salt through Sapphire windows during operation. The center tube (yellow cap) is where the test articles are suspended. For this configuration, the specimens were suspended using an inverted T-shaped nickel trapeze (see Figure 3, which shows the first set of specimens tested, mounted on the trapeze). A seal at the top of this tube allows the trapeze to be raised and lowered using the rod forming the base of the inverted T (at the top of Figure 3). The specimens could therefore be submersed in the salt or raised into the argon cover gas above the salt. In Figure 2, the tube to the left (with two compression fitting caps) allows insertion of two thermocouples for measuring vapor temperature in the cell. The tube with the green cap is where the 3-junction thermocouple probe is inserted to measure salt temperatures. The "Y" shaped tubing to the right is used to maintain an argon purge gas in the cell. During the testing, Argon over-pressure in the cell was maintained at a few psi to ensure that no air could ever enter the cell. The purge tubes are bent upward inside the window ports to maintain a purge gas flow over the inner window surface. (Note that the Sapphire windows are not installed in this picture.) One of the two red-capped tubes is used to exhaust the argon purge gas and the other is a spare port. The tubes were made long enough so that the tops of the tubes would remain at a relatively low temperature. This allowed for Teflon compression type seals to be used. This design requires that the flange be removed (experiment stopped and cooled) in a glove box to access the test specimens.

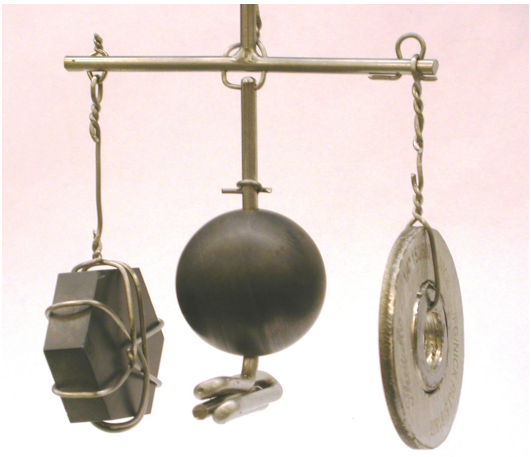

Figure 2. Sample configuration used for first test series.

A second top flange assembly was constructed to allow for specimen retrieval and replacement while the cell remained at temperature. The second top flange assembly

eliminates the need to remove specimens in a glove box. This flange design is shown in Figure 4. A chamber above the valve, which is shown toward the rear of the picture (black knob), allows specimens to be withdrawn from the salt and isolated from the cell using the gate valve. Once the specimens have cooled sufficiently, the port shown in the front of Figure 4 is sealed using a glove bag, the port is opened and the specimens are removed. Insertion of new specimens is done using the reverse of this process. This design requires that the specimens be loaded in a linear string using a series of eyes and hooks to allow for easy specimen removal.

Figure 4. Second top flange assembly.

Figure 5 shows the cell assembly with the first flange design inserted in the furnace. Additional details of the cell design, along with other types of tests performed using this experiment, are presented in Yoder et al. (2014).

2.1 FLiNaK Salt Preparation

Impurities in the fluoride salts increase the corrosion rates in most structural materials (DeVan, 1969). It is therefore necessary to purify these salts before they are used and to maintain the purity of the salts for the duration of operation. This will minimize the corrosion rate and ensure consistent test results.

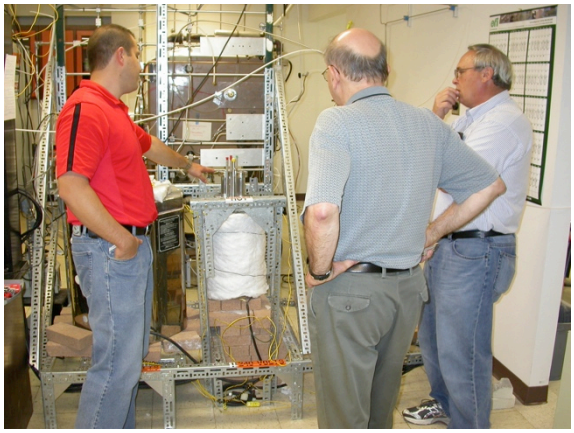

Figure 5. Assembly inserted in furnace.

The purification process used here was originally developed in the MSRE program to purify the initial salt charge and to maintain salt purity throughout the experiment lifetime (Shaffer, 1971). The gas chemistry and filtering process used during salt purification is designed to eliminate any moisture, oxygen, sulfur and tramp metals from the salt.

Commercially available LiF, NaF and KF salts (powder or granular form) were mixed in the appropriate ratios to obtain the eutectic desired. The salt mixture was placed in an open-topped graphite crucible inside a stainless steel vessel to maintain a cover of argon gas over the salt. The purification processing system design is much like the test cell described above except that the top flange design is much simpler. The salt powder was heated and held at a somewhat arbitrary temperature of 300^{o}C for several hours in

order to drive off any moisture while still remaining below the salt melt point (FLiNaK melt temperature is 454°C). After the 300°C soak, salt temperature was raised in order to melt the salt and increase the liquid salt temperature to about 600°C. A mixture of H_2 and HF gas was bubbled through the melt using a dip tube that went through the top flange and penetrated the salt to near the bottom of the melt. The HF/H_2 treatment process was continued for 4–6 weeks to ensure that all oxides, sulfur, etc., were removed. An H_2 purge was then used to sweep all of the HF from the equipment and remove any impurity metal fluorides. Finally, an argon purge was used to remove any hydrogen in the system prior to transferring the salt. After processing, the salt transfer was accomplished by slightly pressurizing the treatment crucible, pushing the salt through a 30 μm nickel frit used to remove insoluble solids (primarily carbon from the graphite processing crucible) and into a storage container.

Transfer of the FLiNaK into the salt cell was accomplished similarly (pressurizing melted salt). Any time the flange was opened (when removing samples, changing flanges, etc.), the entire cell was placed in an argon inerted glove box. Before operation of the cell, to assure the cell was leak free, a 15-50 micron Hg vacuum was pulled on the cell and the cell was isolated for a long enough period to assure that there was no in leakage. Although no direct measurements of salt purity were performed, when observed through the glove box windows, the frozen salt appeared to be very white and clean with a very few small dark specks, presumed to be residual graphite from the processing crucible. When observed in the melted state through the cell windows, the salt appeared to be very clear and transparent.

3.0 Experimentation

Two sets of experiments were conducted: one set using the flange shown in Figure 2 and one using the flange shown in Figure 4. The first experiment used the sample holder shown in Figure 3 and the top flange shown in Figure 2. In the first set of experiments, three different samples were exposed to 700°C salt for 1 month. One of the samples was a piece of Hexoloy® silicon carbide manufactured by Saint-Gobain. This hexagonal piece is on the left of Figure 3. A Poco AXF-5Q machined graphite ball was also tested and is pictured in the center of Figure 3. These graphite balls make up the pebble bed of the LSTL test section. The third specimen was a spiral wound gasket that is used to seal between the silicon carbide flow tube and the remainder of the piping in the LSTL. The Flexitallic gasket is manufactured using alternate layers of grafoil and nickel that are spirally wound to make a compressible seal. The gasket tested is shown on the right side of Figure 3. The three samples were cleaned with alcohol and acetone before testing and inserted in the cell while the cell was in an inert glovebox. The specimens were allowed to hang above the salt in the argon atmosphere as the experiment was heating and were allowed to soak in the argon cover gas for several hours before submerging in the salt. After being submerged in the salt for one month, the specimens were pulled above the salt level in the argon cover gas space using the trapeze, the salt was allowed to freeze, the cover gas was isolated in the cell and the cell was cooled and removed from the furnace and moved to the argon glove box. The top flange of the cell was then removed, allowing removal of the specimens.

Figure 6. Specimens as removed from salt.

Figure 6 shows the specimens inside the glove box as they were removed from the cell. The white covering is salt that remained on the specimens after they were pulled from the liquid salt bath. This covering was easily removed from the specimens using a pencil eraser. The cleaned specimens are shown in Figure 7. Visual inspection of the specimens indicated that that there was no apparent degradation of the material. In fact, machining marks on the graphite sphere were still clearly visible after testing. The specimens were also cross sectioned and microscopically examined. Neither the SiC nor the graphite had any detectable changes. The Flexitallic gasket was cross-sectioned across the diameter of the gasket. Some salt residue was observed between the wound layers, but it could not be determined if this occurred during testing or if it happened during the preparation of the specimen for microscopy. No other degradation was noted either to the nickel or to the grafoil. The backing ring for this seal system was also made of nickel (Figure 7c) and the original markings on the backing ring are still easily seen.

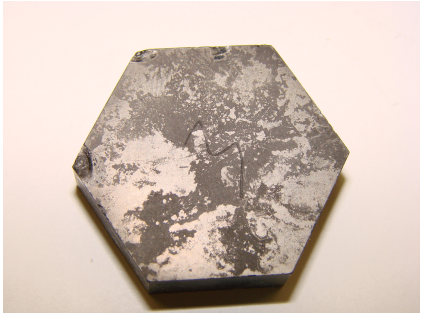

Figure 7a. SiC specimen after cleaning.

Figure 7b. Graphite sphere after cleaning.

Figure 7c. Flexitallic gasket after cleaning.

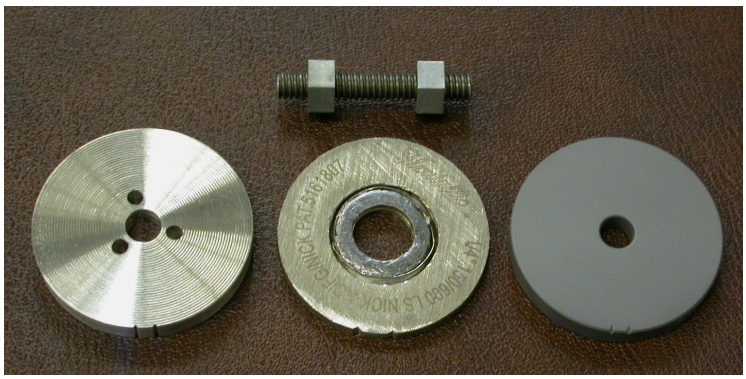

Figure 8. Second specimen set.

A second series of tests was performed to determine if there would be any enhanced material corrosion resulting from two dissimilar materials in contact during salt exposure. A test was performed to simulate the SiC-to-loop sealing system used in the LSTL. This seal uses a SiC flange that is integral to the SiC flow tube. The SiC flange mates to a matching Alloy 600 flange. A Flexitallic gasket sandwiched between the two flanges is used to contain the salt. A small version of this sealing system was tested to ensure that materials were compatible during exposure to salt. A small Flexitallic gasket (grafoil/Ni) was sandwiched between an Alloy 600 disk and a SiC disk (Hexoloy®) using a molybdenum bolt and nuts. Molybdenum was chosen as it has good high temperature properties and excellent corrosion resistance when exposed to fluoride salts. The specimen parts before assembly are shown in Figure 8. The SiC and Alloy 600 disks are 44.5 mm in diameter and 6.35 mm thick. The SiC disk is to the right of the figure, the Flexitallic gasket in the center and the Alloy 600 disk to the left. The Alloy 600 disk has 3 holes drilled in it to allow salt to penetrate into the center hole of the Flexitallic gasket when submerged in the salt. The Flexitallic gasket was compressed before it was sandwiched between the Alloy 600 and SiC disks to prevent overstressing the SiC disk when the three components were bolted together. Three separate sets of these sandwiched components were fabricated to allow three months of testing and specimens to be withdrawn each month. The specimen sets were strung together vertically using nickel wire through holes drilled in the molybdenum bolt. In addition to cleaning with alcohol and acetone, these specimens were hydrogen fired at 700°C for approximately 12 hours in order to remove any oxygen and moisture before testing in salt. Figure 9 shows a photo of the test piece taken through the glove box window after removing it from the test cell.

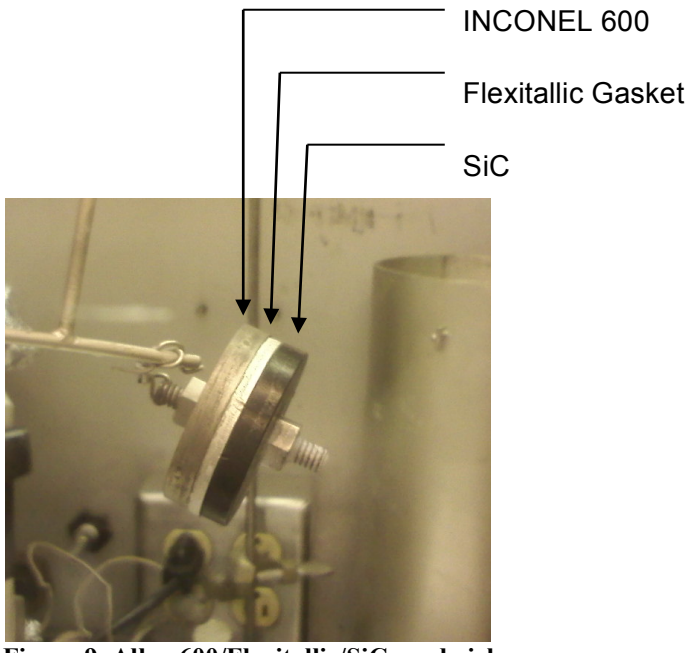

Figure 9. Alloy 600/Flexitallic/SiC sandwich after removal from salt.

3.1 Experimental Results

Figures 10–12 show two surfaces of the SiC disk after 90 days of exposure. Figures 10 and 11 show the surface of the SiC that was in contact with the Flexitallic gasket at two different magnifications. Both figures indicate essentially no degradation of the SiC material. While the etched microstructure shows some variation in sintering, the variability is uniform across the cross section and indicates no attack at the edge of the specimen. Figure 12 shows the SiC surface that was directly in contact with the FLiNaK salt throughout the duration of the 90-day 700°C testing. The 30- and 60-day specimens are not presented in this document since there were essentially no changes in the SiC during testing.

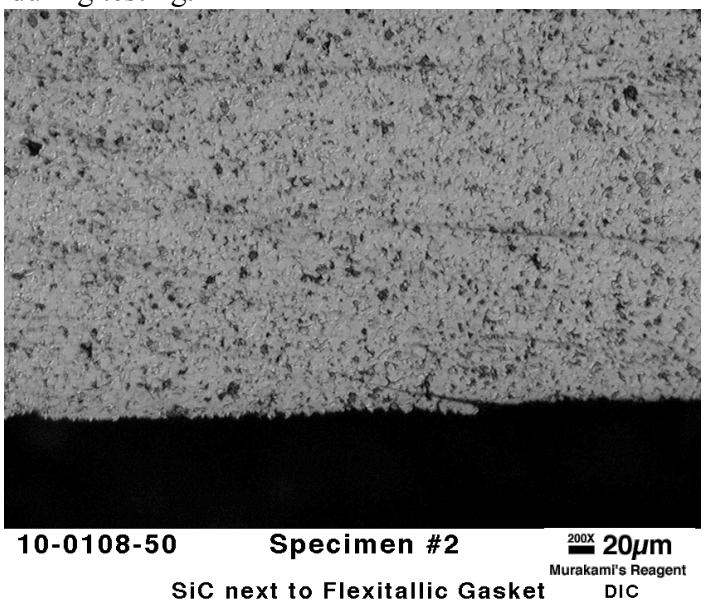

Figure 10. SiC surface next to Flexitallic gasket: 90-day exposure, 200×.

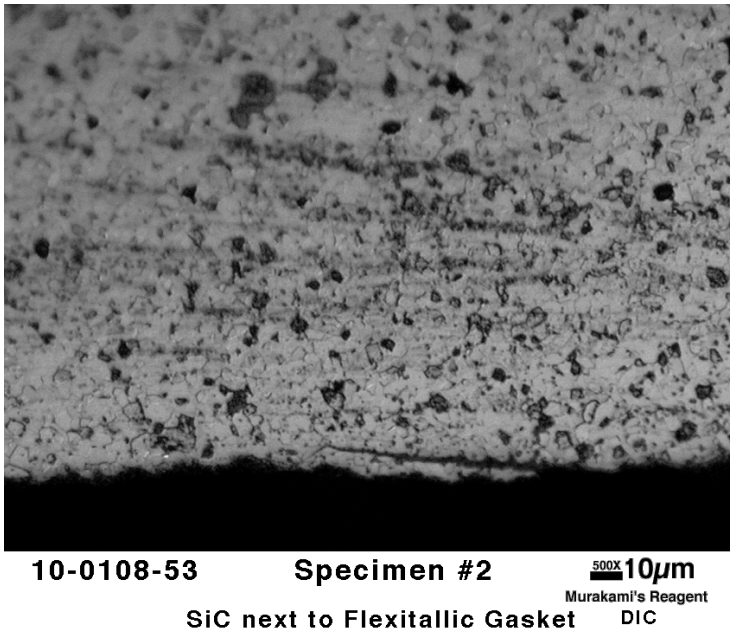

Figure 11. SiC surface next to Flexitallic gasket: 90-day exposure, 500×.

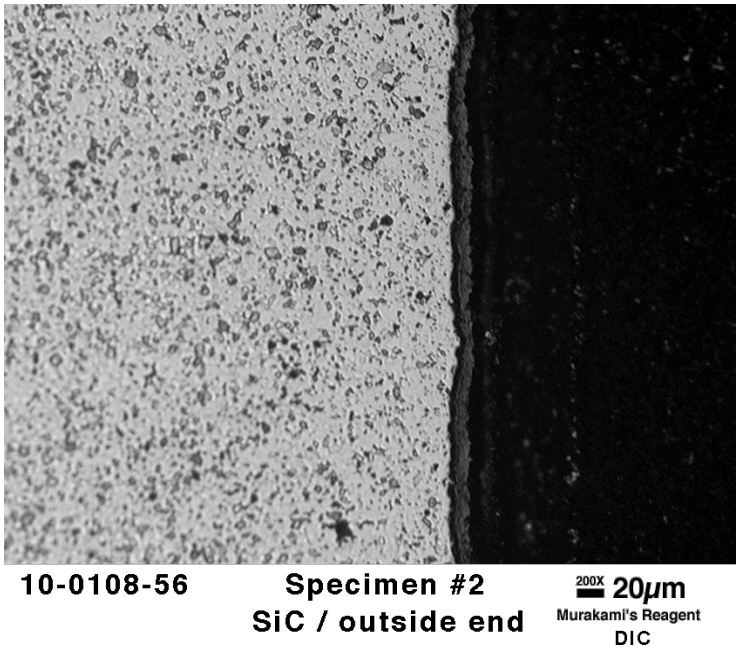

Figure 12. SiC surface: outer diameter directly exposed to salt.

The entire specimen sandwich was cross-sectioned in order to examine the Flexitallic gasket. Micrographs of the Flexitallic gasket specimen that was exposed for 90 days are shown in Figure 13. The micrograph with the lowest magnification (300 μm) shows the spiral portions of the Flexitallic gasket and the grafoil and nickel windings. Also shown in the 300 μm micrograph is a portion of the SiC disk and Alloy 600 disk. The outer nickel backing ring of the Flexitallic gasket is also shown in this micrograph. The intermediate magnification shows only the Flexitallic gasket and it shows a region that appears to have some salt inclusion where salt may have penetrated into the windings. The highest magnification shows details of this inclusion. Inclusions were also observed in several other cross sections. It is not entirely clear if the inclusion occurred during testing or if the salt got into the spiral structure during cross sectioning and preparing the sample. Because the integrity of the spiral was not compromised in other radial locations, it does not appear that the sealing capability of the Flexitallic gasket would be reduced.

Results from the Alloy 600 disk are shown in Figures 14–16. Figure 14 shows the Alloy 600 surface next to the Flexitallic gasket at two different magnifications. This section of the Alloy 600 disk was next to the nickel backing ring of the gasket. The saw-tooth pattern was intentionally machined into the disk in order to simulate an actual flange

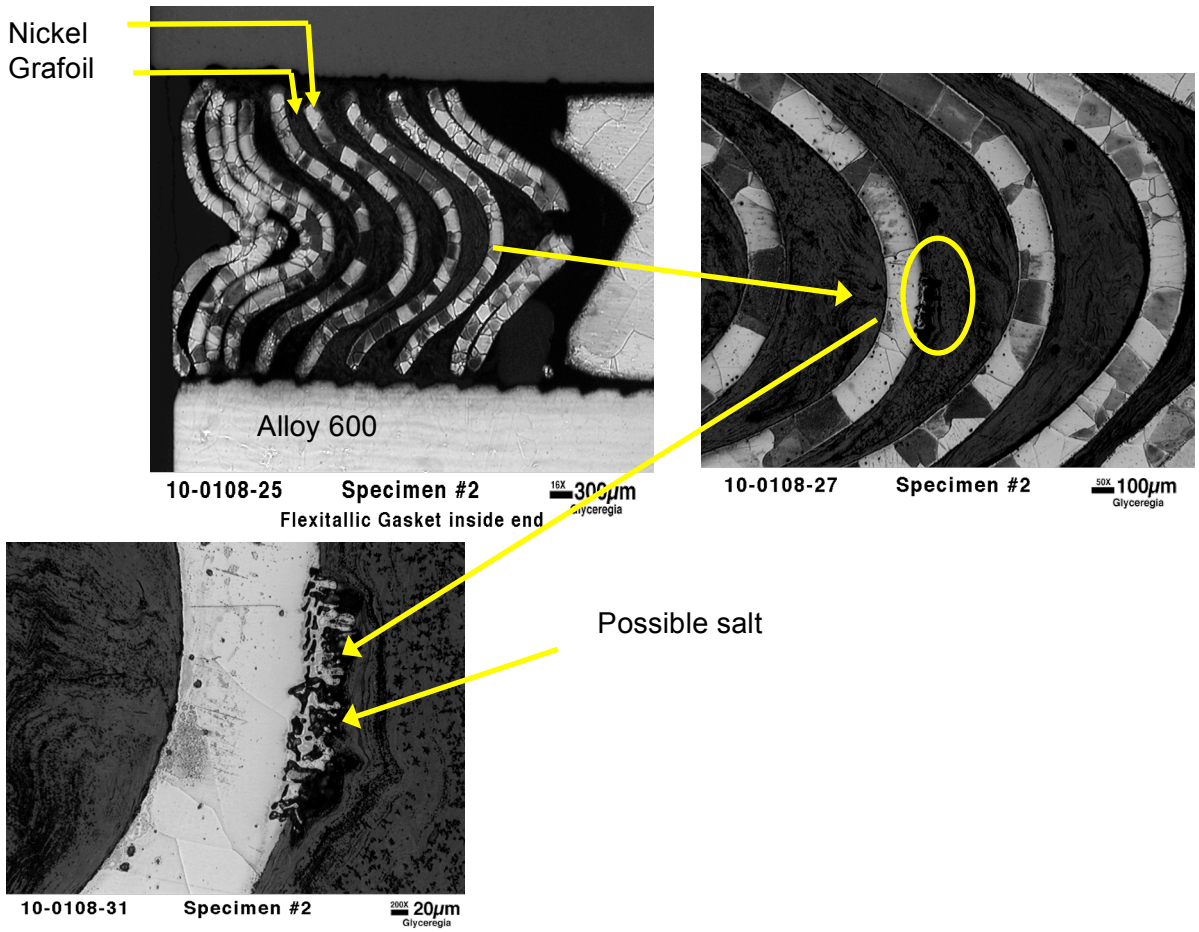

Figure 13. 90-day exposure: Flexitallic gasket.

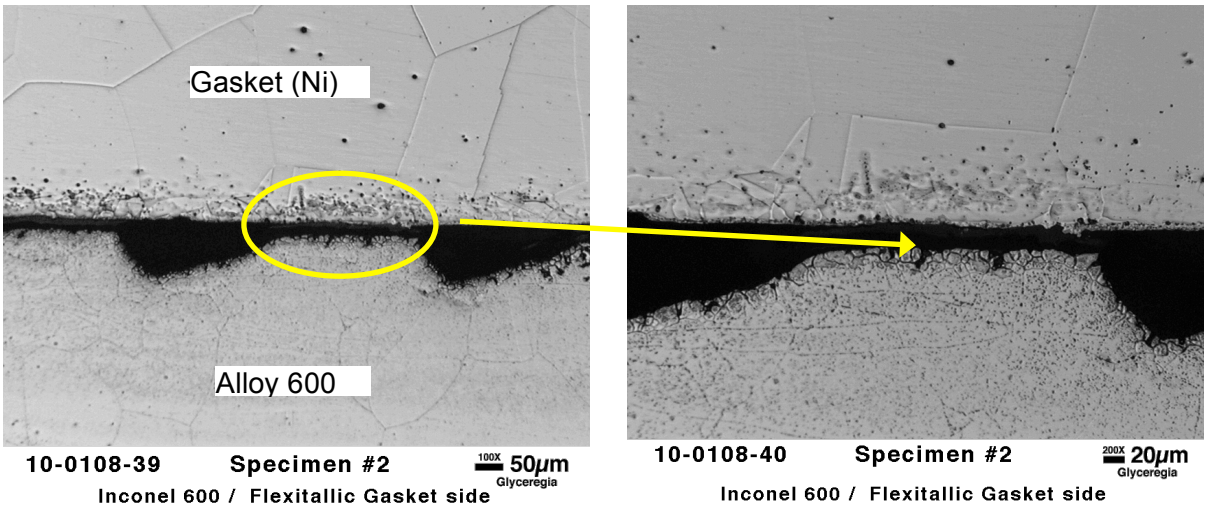

Figure 14. Alloy 600 surface next to Flexitallic gasket.

surface. However, as these two figures indicate, corrosion of this component is evident. Figures 15, 16 and 17 show the Alloy 600 surface at 30-, 60- and 90-day exposure times.

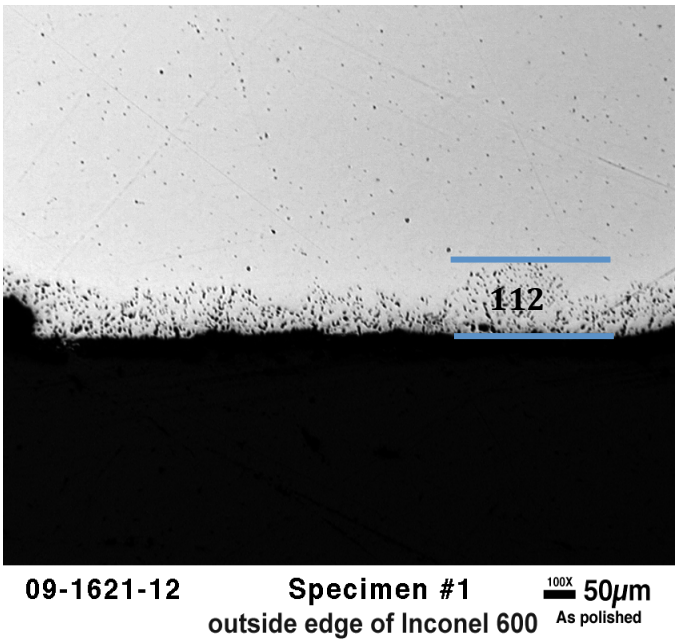

Figure 15. Inconel 600 surface: 60-day exposure.

Previous work (Manly et al., 1957) as part of the Aircraft Nuclear Propulsion (ANP) Program has demonstrated chromium depletion as a mechanism for corrosion of high-chromium nickel-based alloys in fluoride salts. In the tests presented here, corrosion increased with immersion time, as salt volume was great enough so that alloying elements' solubility limits in the melt were not achieved. The outside edge of the specimen showed a corrosion depth of approximately 300 μm after a 90-day exposure. The results of these tests are presented in Figure 18, which shows penetration depth vs. time. as well as results of Manly (1957) who reported natural convection (NC) tests using a fuel salt ($NaF-ZrF_4-UF_4$) in Alloy 600 operating at 815°C. A comparison of the composition of the Manly alloy and the one investigated in this study is shown in Table 1.

Table 1. Specifications of alloy compositions.

Alloy	Elemental Composition (%)								
	Cr	Fe	Mn	C	Al	Ti	S	Si	Ni
Commercial specifications for Alloy 600	14-17	6-10	1 (max)	.15 (max)			.015 (max)	.5 (max)	72 (min)
Manly	15	7	.03	.05	.15	.25		.22	Remainder
Present study	14.58	7.13	.37		<	.26			Remainder
Olson (Alloy 617 – commercial specs)	20-24	3	.5 (max)	.15 (max)	.8-1.5	<.6	.015 (max)	.5 (max)	Remainder

< Indicates less than detection limits

Manly also reported data with Alloy 600 and $NaF-ZrF_4-UF_4$ using forced convection (FC) loop testing at a salt temperature of 870°C, which is also shown in Figure 18. A single data point published by Olson (2009) for Alloy 617 (static corrosion at 850°C salt temperature) is also shown in the figure. Manly's results show higher corrosion rates for the NC tests than the FC tests. High initial corrosion rates are attributable to corrosion cased by impurities in the initial salt charge. Once the impurities in the salt are removed, the corrosion rates reduce, and corrosion (or voiding) is dictated by the chrome depletion process noted above. The initial differences in penetration depth (<~300 hours) between the experiments in Figure 18 are likely due to differences in salt purity in the different experiments. Manly (1957) notes the effect of impurity levels and how they impact consistency of corrosion data. The salt purification process used in the ANP program

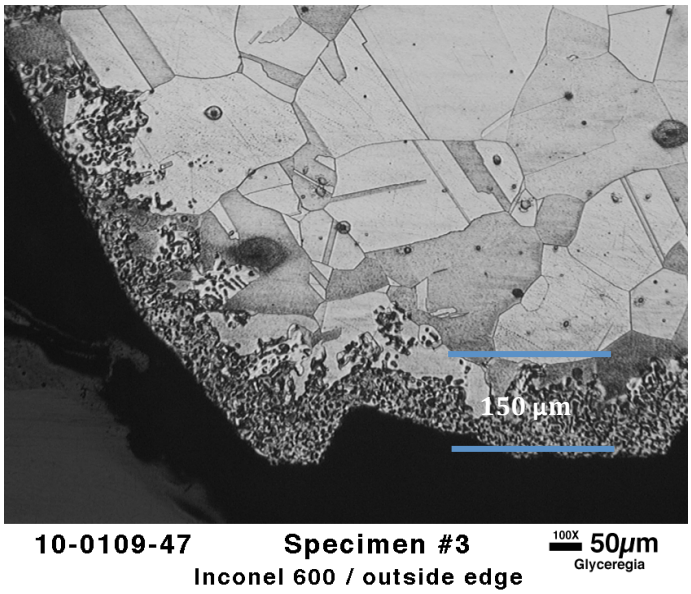

Figure 16. Inconel 600 surface: 60-day exposure.

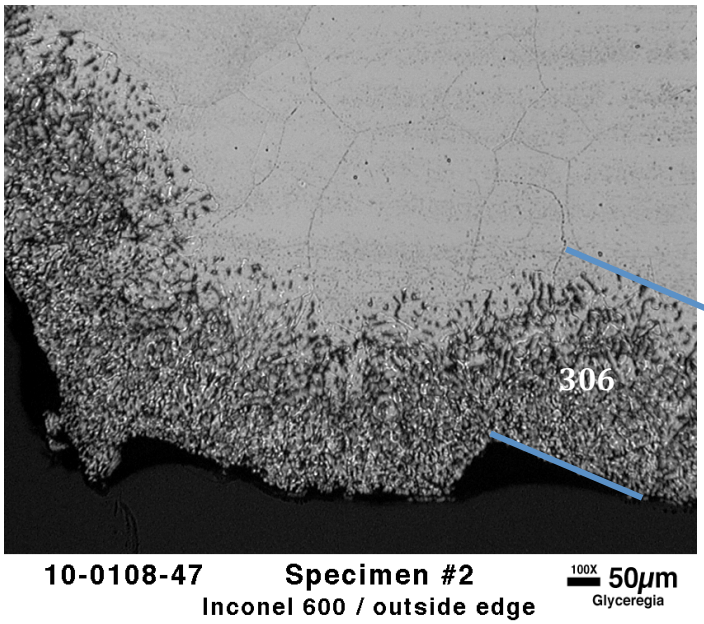

Figure 17. Inconel 600 surface: 90-day exposure.

(Joseph et al., 1954) used a hydrofluorination process, however the hydrofluorination purification process used in the present study used significantly longer purification times than those discussed in the Joseph report, and produce salts with lower impurity levels and therefore would show lower initial corrosion rates.

Slower corrosion rates are observed in Manly's experiments at longer times. Both sets of his data indicate a post impurity corrosion rate of about 0.1µm/h. This corrosion rate is consistent with the present study, and it is expected that corrosion rates in the LSTL will be acceptable as long as salt purity levels are maintained.

The Sapphire windows in the experimental cell were located at the ends of 44.5 mm diameter tubes that extended about 127 mm above the top flange in order to keep them cool. CF type flanges were used to seal the windows located in the argon cover gas space. The windows were designed to allow the salt to be viewed during testing. Figure 19 shows a picture of the specimen through one of the windows. The salt is perfectly clear and one of the Alloy 600 disks can clearly be seen, including the holes drilled in the disk to allow salt to enter the center area of the Flexitallic gasket. Previous experience at lower operating temperatures showed that these windows would stay clear for a long period of time (Yoder, 2014). However, operation at 700°C caused the windows to fog within a few hours of high temperature operation. Figure 20 shows one of the sapphire windows after one day at temperature. As the figure shows, the window has fogged to the point where it can no longer be used for any optical experimentation. This behavior is important because the fluoride salts are transparent to

visible wavelengths and optical techniques may be used to perform inspections, measurements, etc., with the salt remaining a liquid. If windows fog at higher temperatures, these measurements could not be taken.

After corrosion testing was complete, the windows were removed and a sample of the material left on the windows was analyzed to determine its composition. The material was whitish in color and appeared to be a very fine powder that could easily be removed from the window with a paper towel. No degradation or etching of the window was observed. The white material was also found in other areas of the cell that operated at lower temperatures.

Analysis of the fine powder using x-ray diffraction (Figure 21) indicated that this material was a mixture of 39.9% K_3SiF_7, 22.3% K_2SiF_6, 26.5% LiF, 1.5% NaF and 9.7% $NiCrF_6$. The $NiCrF_6$ peaks are very sharp, indicating a crystalline phase. The material consists of several salt components that vaporized and condensed in the lower temperature regions of the cell. Although the SiC sample did not show any apparent corrosion using micrography, it was more likely than not the source of the Si found in the powder.

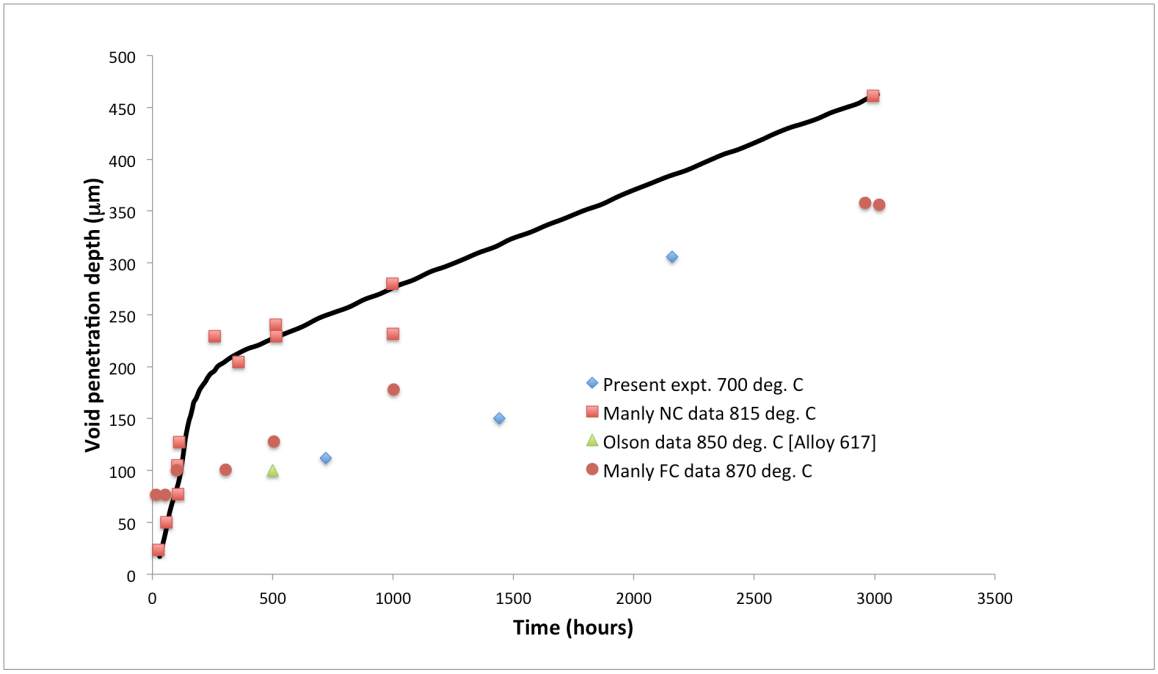

Figure 18. Inconel 600 corrosion rate vs. time.

Figure 19. Specimen submerged in 700°C salt viewed through window.

Figure 20. Sapphire window after one day at 700°C.

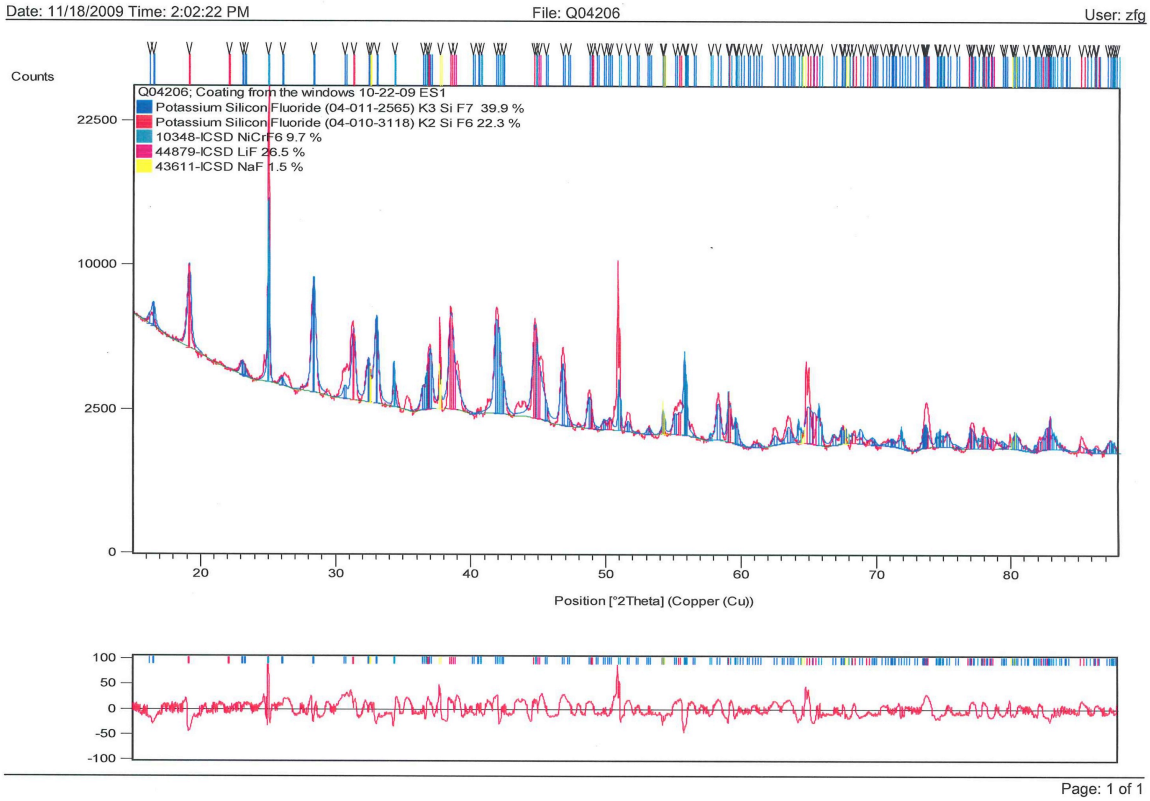

Figure 21. X-ray diffraction analysis of powder on window.

4.0 Conclusions

Three months of FLiNaK corrosion testing has been completed to investigate the behavior of several materials to be used in a liquid salt experimental loop using Hexoloy® SiC (Saint Gobain), Alloy 600, a spiral-wound Flexitallic gasket system and AXF-5Q graphite. All of these materials performed well in the 90-day testing, with only Alloy 600 showing any detectable corrosion.

Alloy 600 showed voiding to a depth of about 300 μm after 90 days of exposure to 700°C FLiNaK salt. The results show that the experimental loop can be safely constructed using these materials and that the facility will have a sufficient operational lifetime. During testing, Sapphire windows in the test cell, which are used for observation of the salt, fogged after only a few hours at high salt temperature. The material fogging the windows was a white powder that could easily be removed. It consisted of components of the salt that condensed in the cooler regions of the cell. Methods of keeping optical ports clear will need to be developed before optical measurement techniques can be used for experimentation or reactor application.

5.0 Bibliography

Bardet, P., et al., "Design, Analysis and Development of the Modular PB-AHTR," *International Congress on Advances in Nuclear Power Plants (ICAPP 2009)*, Curran Associates, NY, May 2009, pp. 161–178.

DeVan, J. H., "Effect of Alloying Additions on Corrosion Behavior of Nickel Molybdenum Alloys in Fused Fluoride Mixtures," ORNL-TM-2021, Oak Ridge National Laboratory, Oak Ridge, TN, May 1969.

DeVan, J. H. and R.B. Evans, III, "Corrosion Behavior of Reactor Materials in Fluoride Salt Mixtures," ORNL-TM-328, Oak Ridge National Laboratory, Oak Ridge, TN, September 1962.

Greene, S.R., et al., "SMAHTR – A Concept for a Small Advanced High Temperature Reactor," *Proceedings of HTR-10*, Prague, Czech Republic, October 18–20, 2010.

Joseph, E. F., et al., "Aircraft Nuclear Propulsion Fluoride Fuel Preparation Facility," ORNL CF-54-6-126, June 29, 1954.

Manly, W. D., et al., "Aircraft Reactor Experiment – Metallurgical Aspects," ORNL-2349, Oak Ridge National Laboratory, Oak Ridge, TN, 1957.

Olson, L. C., et al., "Materials Corrosion in Molten LiF-NaF-KF Salt," *Journal of Fluorine Chemistry*, 130, 67–73, 2009.

Shaffer, J. H., "Preparation and Handling of Salt Mixtures for the Molten Salt Reactor Experiment," ORNL-4616, Oak Ridge National Laboratory, Oak Ridge, TN, 1971.

Uhlir, J., M. Hron, V. Priman, and Z. Frejtich, "Current Status of CZECH R&D Program in Partitioning and Transmutation," http://www.torium.se/res/Documents/uhlirfluorination1.pdf

Varma, V., et al. "AHTR Mechanical, Structural, and Neutronic Preconceptual Design," ORNL/TM-2012/320, Oak Ridge National Laboratory, Oak Ridge, TN, September 2012.

Yoder, G. L., et al., "Development of a Forced-Convection Liquid-Fluoride-Salt Test Loop," *Proceedings of HTR-10*, Prague, Czech Republic, October 18–20, 2010.

Yoder. G. L., et al., "An Experiment to Study Pebble Bed Liquid Fluoride Salt Heat Transfer," *Proceedings of ICAPP 2011*, Nice, France, May 2–5, 2011.

Yoder, G. L., et al., "High-Temperature Fluoride Salt Test Loop," ORNL/TM-2012/430, Oak Ridge National Laboratory, Oak Ridge, TN, September 2012.